Journal of Tethys: Vol. 2, No. 3, 242–253 *ISSN: 2345–2471 ©2014*

Application of AVO Attributes and Fluid Replacement in Determining AVO Anomaly; Case Study of Aboozar Oil Field, Iran

Sadeq Rahim Bakhtiari[1], Ehsan Farahbakhsh[2], Rasoul Hamidzadeh Moghadam[1]

1- Department of Mining Engineering, Sahand University of Technology, Tabriz, Iran.
2- Mining Engineering School, College of Engineering, University of Tehran, Tehran, Iran.

* Corresponding Author: s_rahimbakhtiari@sut.ac.ir

Received: 01 January 2013 / Accepted: 05 August 2014 / Published online: 12 September 2014

Abstract

AVO analysis is a technique which is widely used in industry and is applied on seismic prestack data. Results from changes in seismic wave reflection amplitude versus offset can be used in extracting elastic properties and hence lithology and reservoirs pore fluid identification. Before performing AVO analysis studies, processing steps should be ensured that changes in reflection amplitude are relative to only changes in elastic properties of layers. One of the major parts of AVO analysis is investigation of common AVO attributes such as AVO intercept, AVO gradient and scaled Poisson's ratio and their combinations. The crossplot of AVO attributes can play an efficient role in AVO analysis. In this research, AVO analysis is executed on a loose and unconsolidated sandstone reservoir and also well logging data were used to calibrate real seismic data. By using Fluid Replacement Modeling (FRM) and Gassmann's equation on reservoir well data, AVO behavior in every conditions of reservoir (with changes in fluid type and saturation) shows that it belongs to class IV of Rutherford and William's classification. Moreover, hydrocarbon zones which are defined using applying AVO attributes on cross-sections and target horizon, are found consistent with information from well data.

Keywords: Modeling, Fluid Replacement Modeling, Amplitude versus Offset, AVO Attributes, AVO Attributes Cross Plots.

1–Introduction

Seismic reflection method has been used in hydrocarbon reservoirs investigation since 1930. In seismic data interpretation, quantitative methods have been gradually used instead of qualitative methods in exploration industry. According to different characteristics of compressional (P) and shear waves (S) and different effects of earth elastic properties on these waves, it is necessary to be aware of the shear wave behavior and its changes in addition to P-wave to do quantitative study and obtaining information in the case of different fluids and type of rocks forming materials. (Aki and Richards, 1980).

Reflected wave pulse characteristics variation which originates from a reflector can be interpreted to specify a basin history, rock type in a layer and even pore fluid (Chiburis *et al.*, 1993). Bright spots were first practical evidences to identify fluid existence which were considered in early 1970 especially in identifying gas. But drillings were carried out later on showed that hydrocarbons are not the only source of this amplitude response type. Rutherford and Williams (1989) (Zhang and Brown, 2001) classified amplitude response of gas sands surrounded by shales in seismic sections into three classes for better identification. With further investigations and observing other behaviors from gas sands by

Castagna *et al*. (1989), this classification was developed and fourth type of this response was added to the classification. AVO anomalies classification was not limited to that and later, Castagna and Swan (1997) noted that AVO anomaly investigation using cross plotting of intercept and gradient attributes of AVO would be better. The advantage of using this type of plotting is that much information is available and trends are visible in the data which is not visible in a plot of standard offset (or angle) versus amplitude. AVO analysis investigates variation of reflection and transmission coefficients with angle of incidence in seismic data. Rock properties and corresponding AVO responses can be determined from well-log data in AVO modeling (synthetic model) based on the seismic rock properties which are directly related to seismic wave propagation and seismic responses. Thus for determining anomaly precision caused by changes in lithology or fluid, the main key of using AVO is comparing the existing real data with a standard condition such as a synthetic seismic model.

2– AVO Principles

Reflection and transmission coefficient changes with incidence angle (and corresponding to that offset changes) (AVA) often refer to reflection dependence on offset and is the basis of amplitude analysis versus offset (AVO). Nowadays AVO is widely used in identifying hydrocarbons, lithology determination and fluid parameter analysis based on the fact that seismic amplitudes in boundaries are affected by different physical properties of upper and lower parts of the interface.

When a P wave incident obliquely to an interface of two homogeneous and isotropic layers with unlimited extension and variable acoustic impedance, reflected and refracted P wave is generated similar to normal incidence and moreover some of incident compressed wave energy changes into reflection and refraction of S wave rays (Figure 1).

Reflection and transmission incidence angles of rays based on Snell's law are defined as below:

$$P = \frac{sin\theta_1}{V_{P1}} = \frac{sin\theta_2}{V_{P2}} = \frac{sin\emptyset_1}{V_{S1}} = \frac{sin\emptyset_2}{V_{S2}} \quad (1)$$

In which P is ray parameter.

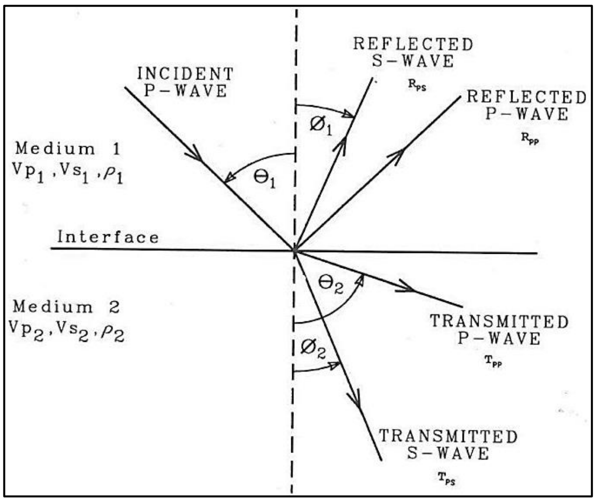

Figure 1) Reflected and refracted rays of P and S waves caused by oblique incident of P wave to an interface with different acoustic impedance at upper and lower parts (Zhang and Brown, 2001).

Knott (1899) and Zoeppritz (1919) invoked continuity of displacement and stress in reflectors as boundary conditions to determine reflection and transmission coefficients as a function of incidence angle and elastic properties of media (density, shear and volumetric module). Zoeppritz's equations describe relations between transmitted, reflected and refracted shear and compressed waves for both media and determines propagation of each ideal flat wave. Reflection and transmission coefficients including $T_{PS}, T_{PP}, R_{PS}, R_{PP}$ in each radiation angle of θ are completely determined by density and wave velocity of P and S in each media. These parameters are themselves depended on physical properties of media such as lithology, porosity and fluid type.

Due to complicated form of Zoeppritz's equations and this fact that they do not give us an intuition of how amplitudes are related to the various physical parameters, Zoeppritz's equations are approximated. Aki and Richards equation (1980) (equation 2) and Shuey's equation (1985) (equation 3) can be mentioned as some of these approximations which simplified the relation between reflection coefficient and incidence angle so that basic coefficients of Zoeppritz can be recognizable.

$$R(\theta) = \frac{1}{2}\left[\frac{\Delta V_P}{V_P} + \frac{\Delta\rho}{\rho}\right]\left[\frac{1}{2}\frac{\Delta V_P}{V_P} - 4\frac{V_S^2}{V_P^2}\frac{\Delta V_S}{V_S} - 2\frac{V_S^2}{V_P^2}\frac{\Delta\rho}{\rho}\right] sin^2\theta + \frac{1}{2}\frac{\Delta V_P}{V_P}[tan^2\theta - sin^3\theta] \quad (2)$$

$$R(\theta) = \frac{1}{2}\left[1 - 4\frac{V_S^2}{V_P^2} sin^2\right]\frac{\Delta\rho}{\rho} + \frac{sec^2\theta}{2}\frac{\Delta V_P}{V_P} - \frac{4V_S^2}{V_P^2} sin^2\theta \quad (3)$$

In which V_P , V_S and ρ are respectively compressional and shear waves average velocity and density in upper and lower medias of interface. Aki-Richards equation is an appropriate approximation of Zoeppritz's equation in angles less than 30 degrees (can be used even with angle larger than 30 degrees). Also Shuey's equation can be changed as equation 4 (Castagna, 1993).

$$R(\theta) = R_0 + \left[A_0 R_0 + \frac{\Delta\sigma}{(1-\sigma)^2}\right] sin^2\theta + \frac{1}{2}\frac{\Delta V_P}{V_P}(tan^2\theta + sin^2\theta) \quad (4)$$

Where R_0 is normal reflection coefficient of P-wave and A_0, $\Delta\sigma$ and σ are respectively defined as below:

$$A_0 = B_0 - 2(1 + B_0)\frac{1-2\sigma}{1-\sigma}, B_0 = \frac{\Delta V_P/V_P}{\Delta V_P/V_P + \Delta\rho/\rho} \quad (5)$$

$$\sigma = (\sigma_2 + \sigma_1)/2, \Delta\sigma = \sigma_2 - \sigma_1 \quad (6)$$

Where ΔV_ρ and $\Delta\rho$ are respectively changes of P-wave velocity and density in interfaces and V_P and ρ are average velocity of P- wave and density.

Difference of V_P/V_S or Poisson's ratio in interfaces cause changes in reflection coefficients versus incidence angle. Relation of Poisson's ratio with seismic wave velocities is expressed as below (Ostrander, 1984):

$$\sigma = \frac{\frac{1}{2}\left(\frac{V_P}{V_S}\right)^2 - 1}{\left(\frac{V_P}{V_S}\right)^2 - 1} \quad (7)$$

3– AVO Classification

Early practical evidence that fluids could be seen by seismic waves as bright spots was often used to identify gas. Bright spots were recognized in the early 1970s as potential hydrocarbon indicators, but drillers soon learned that hydrocarbons are not the only generator of bright spots. Only AVO analysis which requires special data can distinguish lithology changes from fluid changes (Chiburis *et al*., 1993).

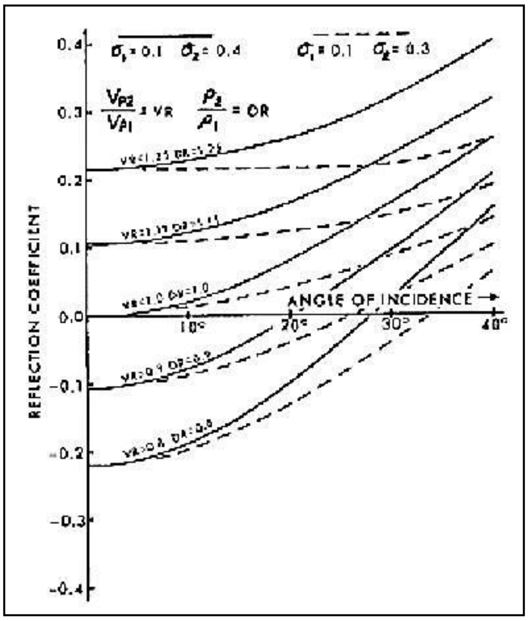

Figure 2) Plot of P-wave reflection coefficient versus incidence angle for an increase in Poisson's ratios across an interface (Ostrander, 1984).

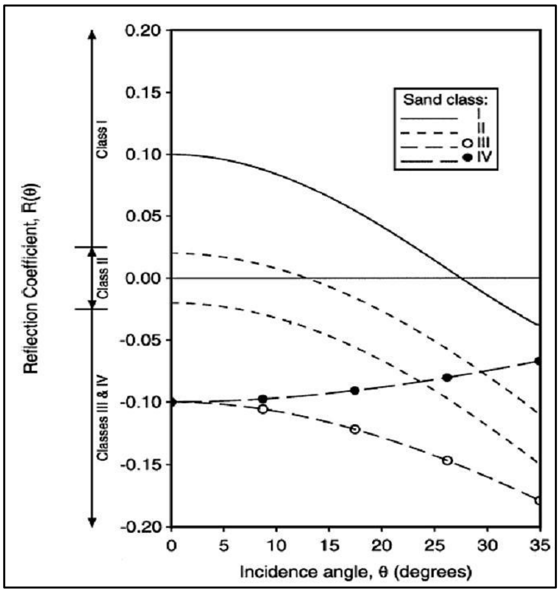

Fig. 3. AVO response curves related to gas saturated clastic reservoirs with shale cap rock; in this figure, reflection coefficients changes versus incidence angle are observed in four AVO classes. Class I has a positive normal reflection coefficient and a negative gradient, class II has a small normal reflection coefficient near zero and class III has a negative normal reflection coefficient and a negative gradient (Rutherford and Williams 1989). Class IV includes negative normal reflection coefficient but

positive gradient, hence amplitude decreases with increasing offset (Castagna et al., 1998).

Rutherford and Williams (1989) classified different responses of gas sand reservoirs. They divided these gas sands reflections according to value of normal incidence reflection coefficient (R_0) at the top of gas sands into three groups. Figure 3 shows reflection coefficients changes versus incidence angle from shale to gas sand. As can be seen, changes include sands with high acoustic impedance (class I), sands with acoustic impedance near shale (class II) and sands with low acoustic impedance (class III). Castagna and Swan (1997) introduced fourth type of AVO changes (class IV). In this class, normal reflection coefficient is negative and while offset increases, its absolute value decreases.

4– Fluid Replacement Modeling

Changing of fluid type and its saturation value at reservoir and creating synthetic logs relating to these changes is introduced as fluid replacement modeling. In most cases, only one well data is available in study area which has encountered with a specified horizon (oil, gas or water). In such situation, modeling of AVO behavior for all conditions of reservoir including gas, oil and water is not possible. The solution is modeling of reservoir rock and existing fluids, and then prediction of synthetic logs with substituting fluid type using this modeling. By having P-wave logs, shear wave and density and using Zoeppritz's equations or one of its approximations, AVO behavior of reservoir can be estimated in different conditions of pore fluid and comparing that with seismic data through providing synthetic seismograph. Gassmann's equations (1951) are used to model reservoir rock. Gassmann performed equation 8 to predict reservoir seismic properties changes (density, compressional and shear wave velocity) caused by fluid replacement based on texture property of reservoir rock.

$$K = K_{dry} + \frac{\left(1-\frac{K_{dry}}{K_m}\right)^2}{\frac{Q}{K_f}+\frac{1-Q}{K_m}+\frac{K_{dry}}{K_m^2}} \qquad (8)$$

In which K is volumetric module of saturated reservoir rock of a fluid with volumetric module of K_f and K_{dry} is volumetric module of rock frame in dry condition. K_m is volumetric module resultant of forming minerals in reservoir rock and Q is reservoir rock porosity.

5– AVO Attributes

AVO interpretation basically is extracting AVO common attributes including intercept (A), gradient (B), and pseudo Poisson's ratio and cross plotting them to specify reservoir fluids and different lithological units. Cross plotting in AVO can be used to determine AVO class (Foster and Keys, 1999; Castagna and Swan, 1997) and identifying hydrocarbon sediments (Ross and Kinmann, 1995; Verm and Hilterman, 1995). Under different geological conditions, A and B values in water sands and shale layers follow a specific trend of background (figure 4). AVO anomaly is a deviation from this trend of background that may be related to lithology factors or hydrocarbon presence. Gradient of this line depends on V_P/V_S ratio of background.

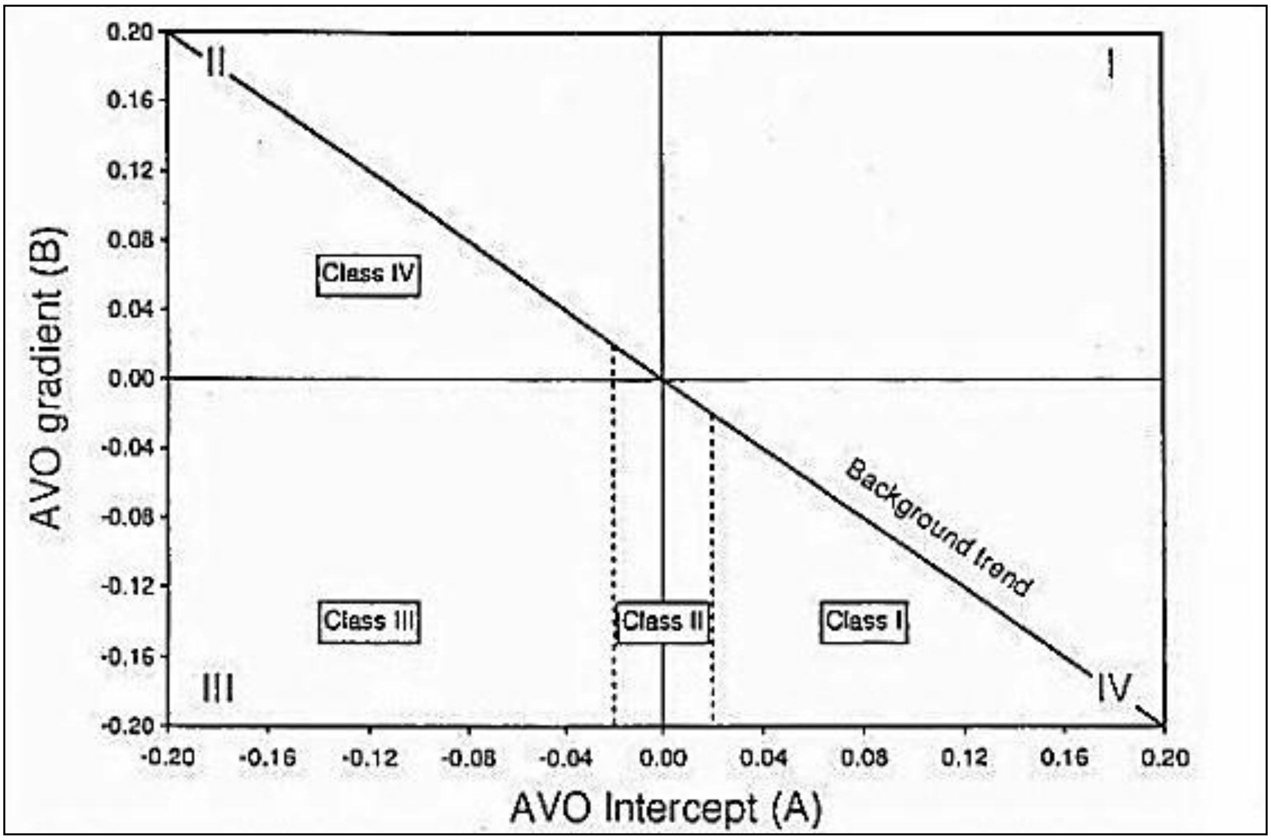

Figure 4) Cross plotting of intercept (A) and gradient (B) shows existence possibility of four changing areas depending on intercept and gradient. Situation of each one of AVO classes in these areas has been specified. For a limited timing window, water sand and shale locate over a specified background trend. Top of gas layer locates in lower part of background trend and the end of gas layer at the upper trend part (Castagna et al., 1998).

6– Case Study

6.1- Field Information

Case study was done on a filed located in Persian Gulf with 242 square kilometers area and reservoir depth between 820 to 880 meters. Hydrocarbon in this field originates from an oligo-miocene sandstone formation. Field is an anticline with trend of NW-SE and plunge of 1 to 1.5 degrees which has a hydrocarbon column with a length of 62 meters from the top. Reservoir includes oil column of roughly 44 meters and a gas cap with maximum 18 meters. Field includes 3 units: lower carbonated Asmari, Ghar sand (equivalent to Ahwaz section) and upper carbonated Asmari (lower Fars). Upper Asmari includes reservoir potential while lower Asmari is completely consolidated and with no porosity.

6.2- Processing

Considered well penetrates the reservoir at oil containing position therefore by using fluid replacement method, other conditions (place as gas or water saturated) were modeled. In figure 8, shear and compressional wave logs and density for each three conditions of pore fluid presence can be observed. As considered, ΔV_P and ΔV_S are negative in all conditions (oil, gas and water) so based on equation 2, normal reflection coefficient (R_0) is negative and $R(\theta)$ should be positive so total increasing of amplitude versus offset should be decreased.

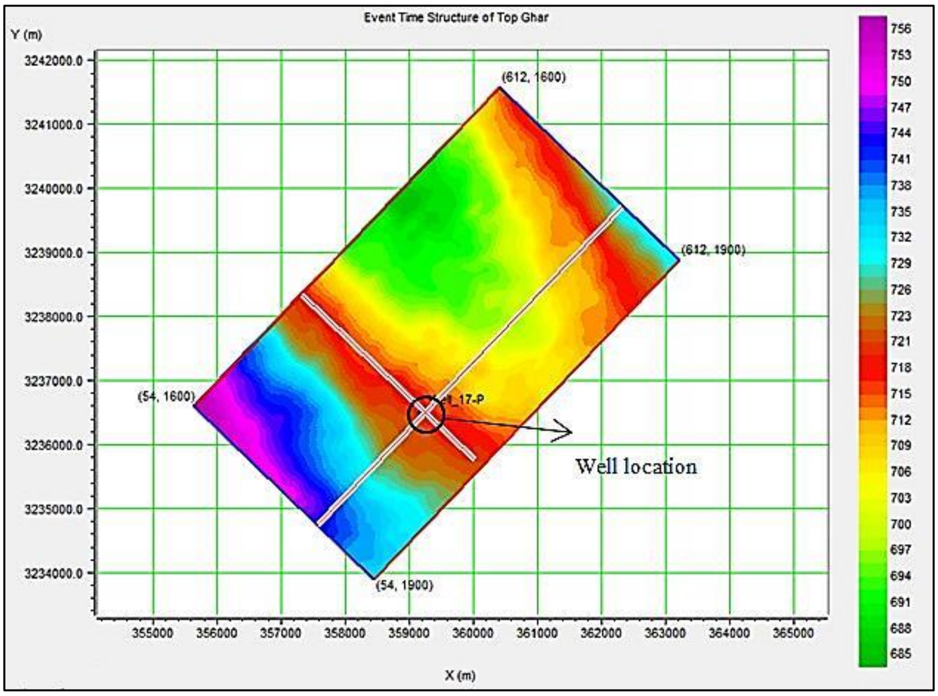

Figure 5) Time changes of reservoir upper horizon (time decreases from violet to green) and well location.

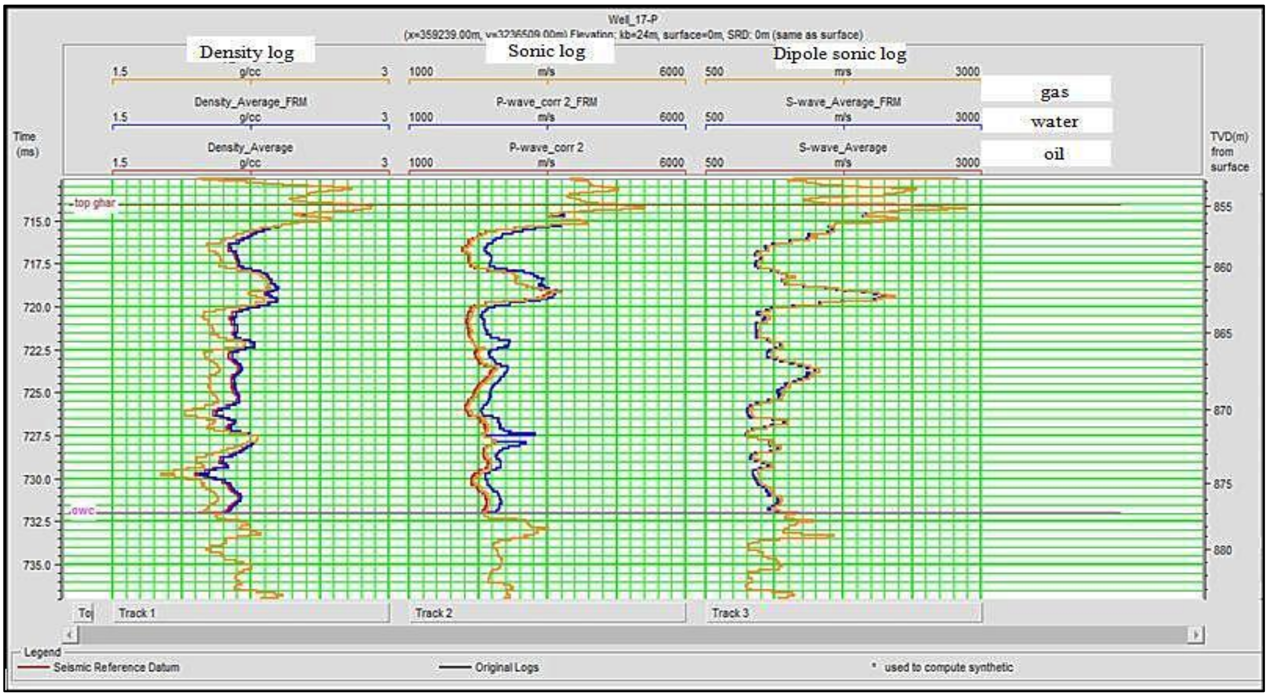

Figure 6) Changes of Vp, Vs and density caused by fluid type changing at reservoir which has been performed by fluid replacement modeling using well data (orange, red and blue logs respectively refers to gas, oil and water saturated conditions). Density and compressional wave logs in water saturated condition (at the top of reservoir) is maximum and in gas saturated condition is minimum while shear wave log in gas saturated is a few more than two other conditions.

It should be noted that because of negative phase of wavelet used in modeling (because of using reverse polarity in processing of seismic data), intercept in Figure 7 is positive and gradient is negative (if phase being normal, intercept and gradient will respectively be negative and positive then AVO anomaly shows class IV). In figure 8, stacked seismic section from the attribute of scaled Poisson’s ratio in upper horizon of reservoir related to synthetic CDP gathers in Figure 7 is observed. As can be seen, amount of scaled Poisson’s ratio variations in gas saturated condition is more than other two conditions although difference of gas and oil saturated conditions is not so much. Therefore this attribute can be suitable for the separation of fluids boundary. Also since in each three conditions, gradient is roughly equal but intercept is different, intercept attribute can also be suitable for the separation of fluids border.

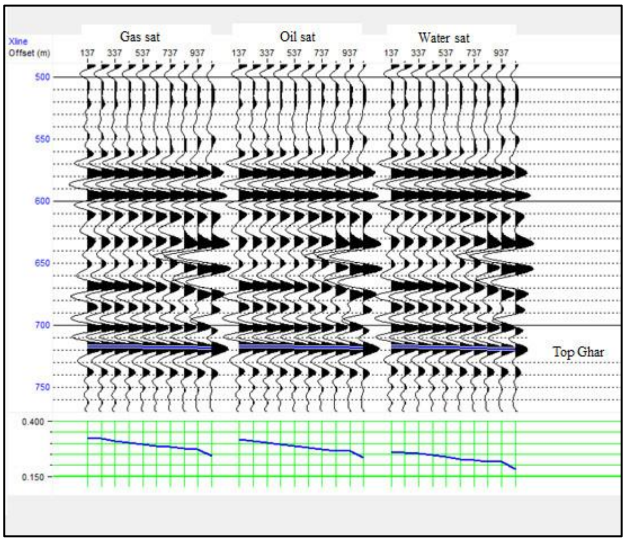

Figure 7) AVO behavior at the top of reservoir relating to synthetic CMP gather with changing fluid type. Gathers are respectively from left to right related to gas, oil and water saturated conditions. In lower part of figure, amount of amplitude versus offset variations is shown.

6.3- AVO Interpretation

As can be seen in figure 9, at the top of reservoir, AVO behavior in seismic data matches AVO behavior gained from well data and AVO class IV can be observed well at this horizon. It is noteworthy that non-uniform variations of amplitude in real data is coming up from noise existence at data but in general there is a linear trend similar to AVO behavior in synthetic model.

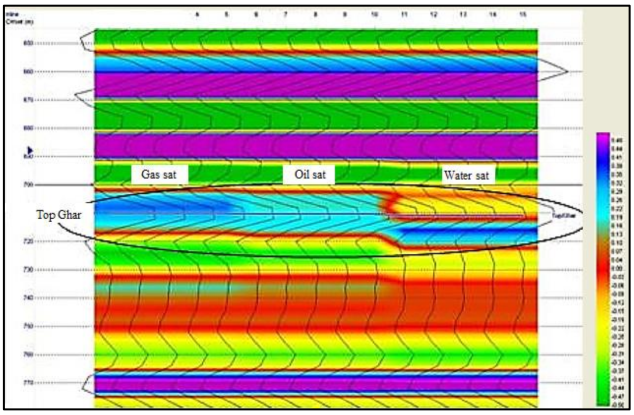

Figure 8) Stacked section of scaled Poisson's ratio related to gathers in figure 7. From left to right, seismic effects are respectively related to gas, oil and water saturated conditions (Mirzakhanian, 2007).

After extracting attributes (Figs. 10, 11 and 12) using cross plotting of intercept versus gradient and gradient versus scaled Poisson's ratio for synthetic model as a pattern and applying that as anomaly zones (red color) and background (grey color) on resulted cross plotting from real seismic data, lateral section is gained in which upper horizon can be observed well (Figs. 13 and 14).

As can be seen at Figures 15, 16 and 17, fluid changing can be observed well at top of reservoir and where top horizon of reservoir crossing well site, based on intercept, gradient and scaled Poisson's ratio.

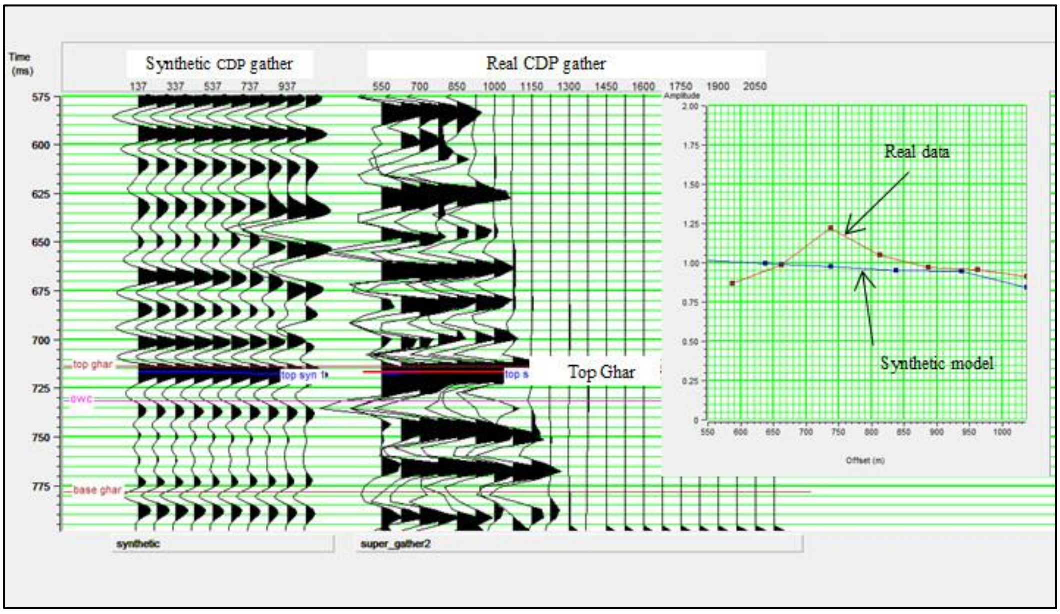

Figure 9) Comparing AVO at top of reservoir for synthetic model and seismic data (In right figure, red line shows amplitude changes in real data and blue line refers to amplitude changes in synthetic model).

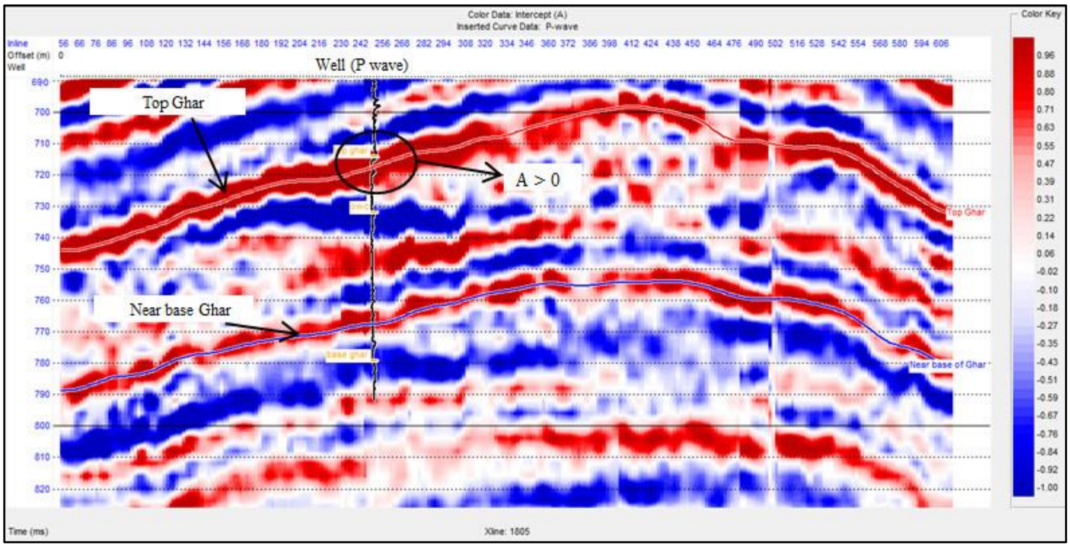

Figure 10) Cross section of intercept attribute (A) at well place. AVO intercept at top of horizon is positive.

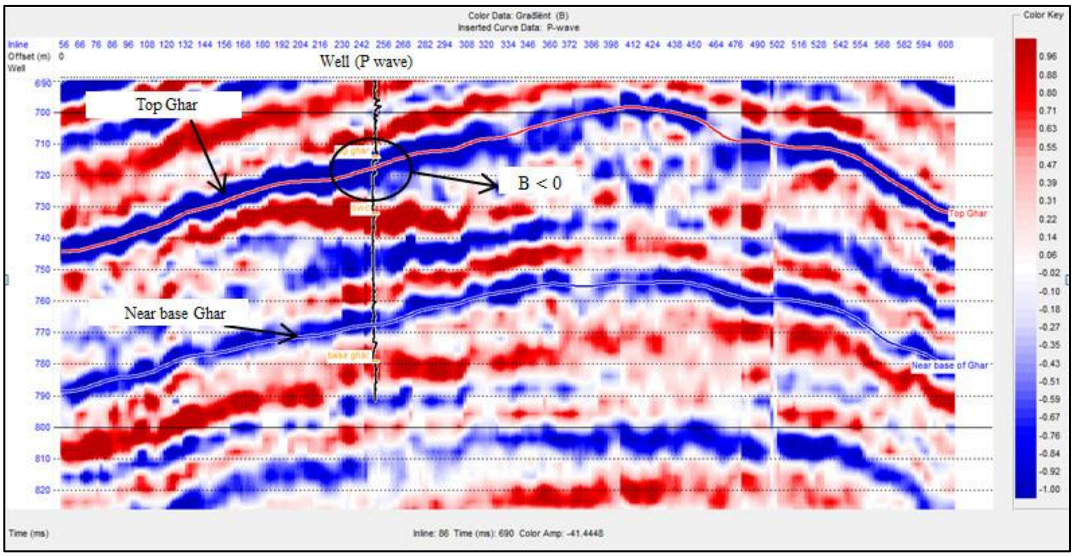

Figure 11) Cross section of gradient attribute (B) passes across a well. AVO gradient at top of horizon is negative.

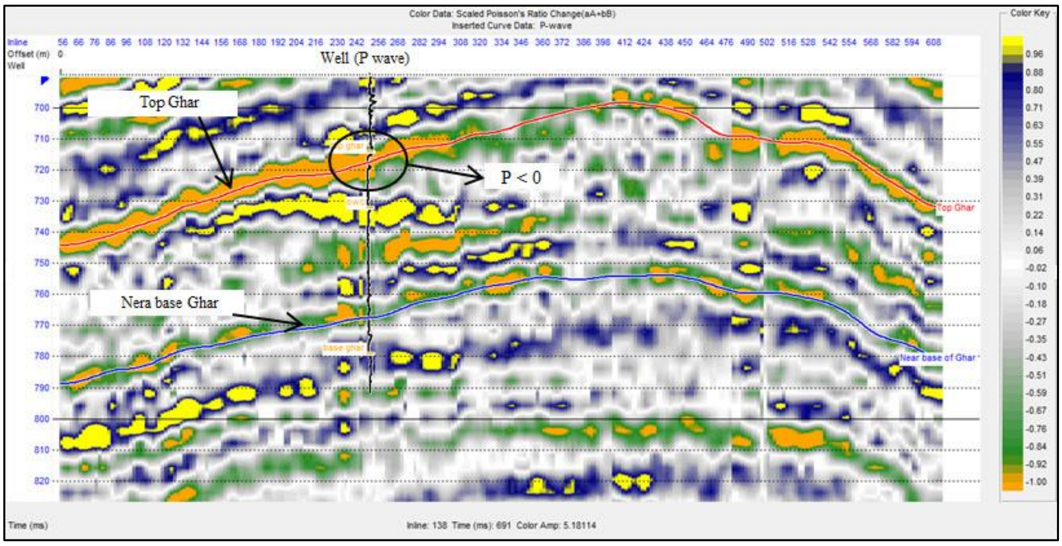

Figure 12) Cross section of scaled Poisson's ratio passes through well.

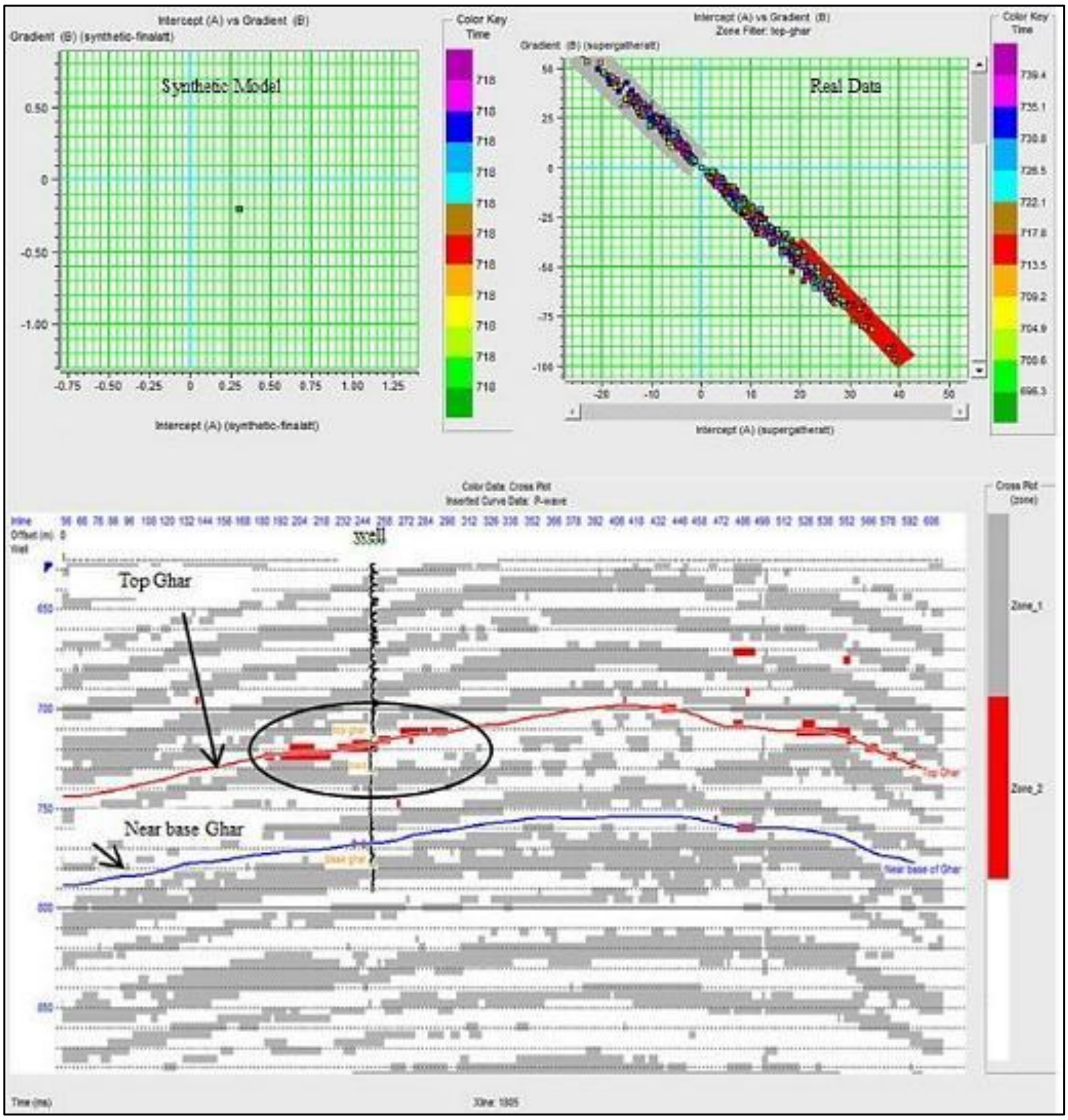

Figure 13) Cross plotting of intercept and gradient attributes at upper horizon of reservoir for synthetic model (upper left) and for seismic data (upper right) and also seismic data cross section caused by their cross plot zoning (lower).

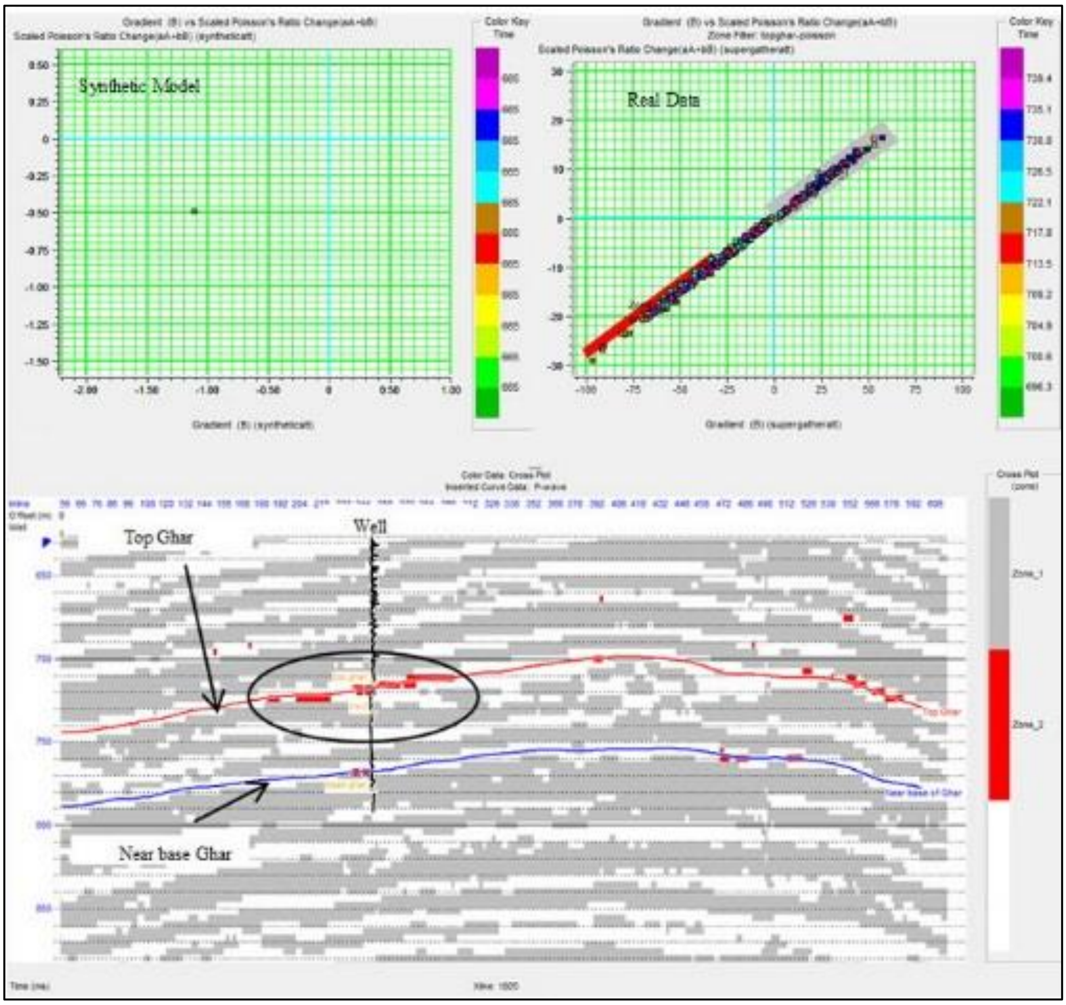

Figure 14) Cross plotting of scaled Poisson's ratio and gradient attributes of AVO at upper horizon of reservoir for synthetic model (upper left) and for seismic data (upper right) and also seismic data cross section caused by their cross plot zoning (lower).

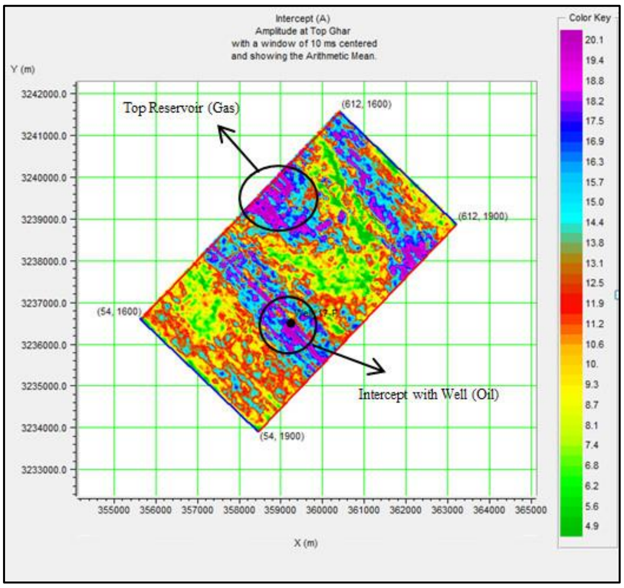

Figure 15) Intercept attribute of AVO at upper horizon of reservoir resulted by arithmetic average.

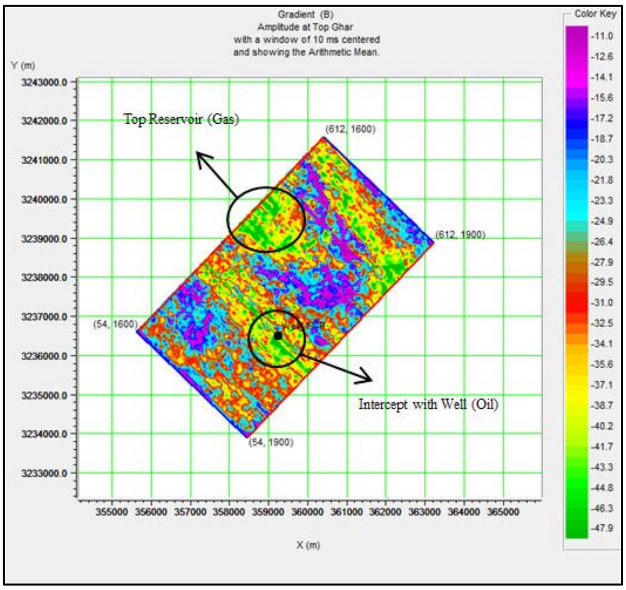

Figure 16) Gradient attribute of AVO at upper horizon of reservoir resulted by arithmetic average.

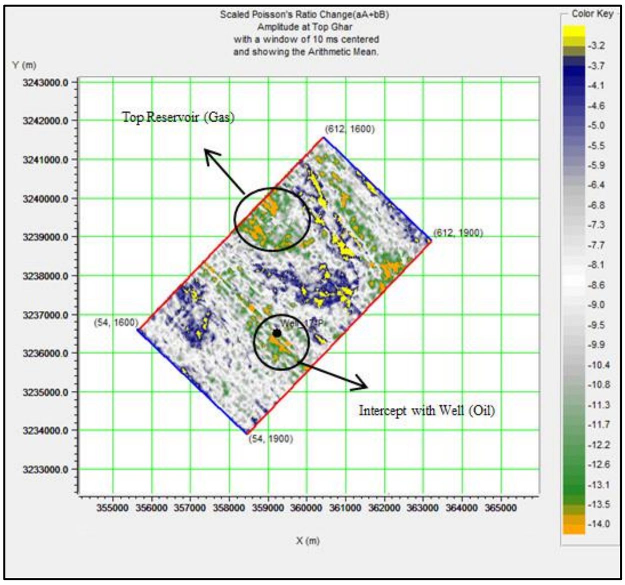

Figure 17) Scaled Poisson's ratio attribute of AVO at upper horizon of reservoir resulted by arithmetic average.

7– Conclusions

In this research, AVO studies were done on one of the oil fields located at Persian Gulf. To investigate the reservoir AVO changes at different conditions, reservoir fluid modeling was performed using Gassmann's equation and synthetic logs of P and S wave velocity and density for water and gas saturated reservoir conditions. By this modeling, AVO behavior and class are specified at the top of reservoir. Then, AVO analysis was run on 3D seismic data. Due to difference in acoustic impedance between cap rock and reservoir sandstone, top horizon of reservoir at seismic section can be identified as a specified horizon with negative reflection coefficient (that appears like a peak due to negative phase of wavelet at processing). The AVO analysis showed that Ghar sand reservoir belongs to class IV. Each one of three reservoir conditions (gas, oil and water saturated) in FRM modeling includes roughly equal gradient, while absolute value of intercept at gas saturated condition is maximum and at water saturated condition has minimum value and at oil saturated condition, because of having some dissolved gas amount of this attribute is near gas saturated. Intercept and scaled Poisson's ratio attributes were evaluated in determining appropriate reservoir fluids. Due to noise existence in real data, intercept attribute at gas and oil saturated conditions is roughly similar; however at upper horizon of reservoir maps related to extracted attributes (Figs. 15,16,17), fluid changing boundary can be specified well.

Acknowledgments:

The authors would like to thank Dr. H. Zhou and Dr. M. Farfour for their appreciate comments which helped us to improve the manuscript.

References:

Aki, K., Richards, P. G. 1980. Quantitative Seismology: Theory and Methods, Volume I: WH Freeman and Co., 700 p.

Alaei, B. 2012. Seismic Modeling of Complex Geological Structures, in: Masaki Kanao (Ed.), Seismic Waves-Research and Analysis. InTech, pp. 213-236.

Castagna, J. P., Backus, M. M. 1993. Offset-Dependent Reflectivity: Theory and Practice of AVO Analysis. Society of Exploration Geophysicists, 348 p.

Castagna, J. P., Swan, H. W., Foster, D. J. 1998. Framework for AVO gradient and intercept interpretation. Journal of Geophysics: 63, 948–956.

Castagna, J., Swan, H. 1997. Principles of AVO crossplotting. Journal of the Leading Edge: 16, 337–342.

Castagna, J., Batzle, M., Eastwood, R. 1985. Relationships between P-wave and shear-wave velocities in clastic silicate rocks. Journal of Geophysics: 50, 571–581.

Castagna, J. P. 2001. Recent advances in seismic lithologic analysis. Journal of Geophysics: 66, 42-46.

Castagna, J. P. Smith, S. W. 1994. Comparison of AVO indicators: A modeling study. Geophysics: 59, 1849–1855.

Chiburis, E., Franck, C., Leaney, S., McHugo, S., Skidmore, C. 1993. Hydrocarbon Detection with AVO. Oilfield Review, 6, 42–50.

Foster, D. J., Keys, R. G., Lane, F. D. 2010. Interpretation of AVO anomalies. Journal of Geophysics: 75, 3–13.

Fatti, J. L., Smith, G. C., Vali, P. J., Strauss, P. J, Levitt, P. R. 1994. Detection of gas in sandstone reservoirs using AVO analysis: a 3-D seismic case history using the Geostack technique. Journal of Geophysics: 59, 1362–1376.

Fugro-Jason (UK) Ltd. 2006. Aboozar field geostatistical inversion report. IOOC.

Gardner, G., Gardner, L., Gregory, A. 1974. Formation velocity and density; the diagnostic basics for stratigraphic traps. Journal of Geophysics: 39, 770–80.

Goodway, B., Chen, T., Downton, J. 1997. Improved AVO fluid detection and lithology discrimination using Lame petrophysical parameters. 67th Annual International Meeting (Society of Exploration Geophysics), 183–186.

Goodway, B. 2001. A tutorial on AVO and Lame constants for rock parameterization and fluid detection. Journal of CSEG Recorder: 26, 39–60.

Kearey, P., Brooks, M., Hill, I. 2002. An Introduction to Geophysical Exploration, third ed. John Wiley and Sons, 272 p.

Knott, C. 1899. Reflection and refraction of elastic waves with seismological applications. Philosophy Magazine: 48, 64–97.

Mirzakhanian, M., Javaherian, A. 2007. Segregation of reservoir fluids and different lithology in Ghar sandstone reservoir in Aboozar oil field of Persian Gulf using AVO attributes. 13th Conference of Geophysics, Iran [In Persian].

Ostrander, W. J. 1984. Plane wave reflection coefficients for gas sands at non-normal angles of incident. Journal of Geophysics: 49, 1637–1648.

Richards, T. C. 1961. Motion of the ground on arrival of reflected longitudinal and transverse waves at wide-angle reflection distances. Journal of Geophysics: 26, 277–297.

Ross, C. P., Kinmann, D. L. 1995. Non-bright spot AVO; two examples. Journal of Geophysics: 60, 1398–1408.

Russell, B., Line, L. R., Hirsche, K.W., Peron, J. 2000. The AVO modeling volume. Journal of Exploration Geophysics: 32, 264–270.

Rutherford, S., Williams, R. 1989. Amplitude-versus-offset variations in gas sands. Journal of Geophysics: 54, 680–688.

Sheriff, R., Geldart, L. 1995. Exploration Seismology, Second ed. Cambridge University Press, 628 p.

Shuey, R. T. 1985. A simplification of the Zoeppritz equations. Journal of Geophysics: 50, 609–614.

Smith, G. C., Gidlow, P. M. 1987. Weighted stacking for rock property estimation and detection of gas. Journal of Geophysical Prospecting: 35, 993–1014.

Verm, R. W., Hilterman, F. J. 1994. Lithologic color-coded sections by AVO crossplots. 64th Society of Exploration Geophysicists Meeting.

Yilmaz, O. 2001. Seismic data analysis and processing, inversion, and interpretation of seismic data, Second vol. Society of Exploration Geophysicists, 1000 p.

Zhang, H., Brown, R. J. 2001. A review of AVO analysis. CREWES Research Report: 13.

Zoeppritz, K. 1919. Erdbebenwellen VII. VIIb, Über Reflexion und Durchgang seismischer Wellen durch Unstetigkeitsflächen. Nachrichten von der Königlichen Gesellschaft der Wissenschaften zu Göttingen, Mathematisch-physikalische Klasse: 66–84.